
Figures and figure supplements

Force propagation between epithelial cells depends on active coupling and mechano-structural polarization

Artur Ruppel and Dennis Wörthmüller *et al.*

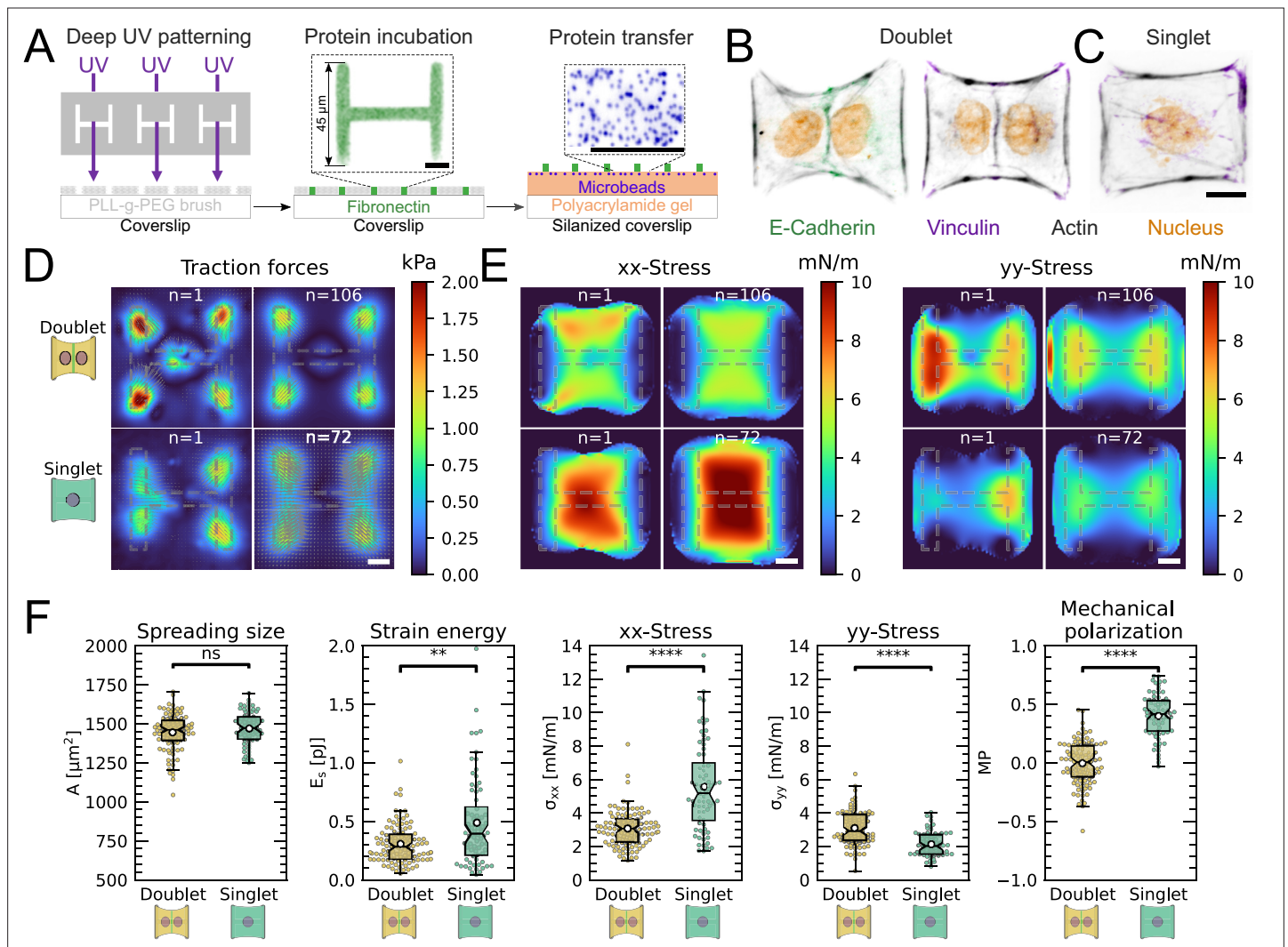


Figure 1. The cell-cell junction leads to a decrease in mechanical polarization. **(A)** Cartoon of the micropatterning process on soft substrates, allowing to control cell shape and measure forces at the same time by embedding fluorescent microbeads into the gel and measuring their displacement. The middle panel shows the used pattern geometry, an H with dimensions of $45\ \mu\text{m} \times 45\ \mu\text{m}$. **(B, C)** Immunostaining of opto-MDCK cells plated on H-patterns and incubated for 24h before fixing. Actin is shown in black, E-cadherin in green, vinculin in violet, and the nucleus in orange. **(B)** The left and right images show a representative example of a doublet. **(C)** A representative example of a singlet. **(D)** Traction stress and force maps of doublets (top) and singlets (bottom) with a representative example on the left and an average on the right. **(E)** Cell stress maps calculated by applying a monolayer stress microscopy algorithm to the traction stress maps, with a representative example on the left and an average on the right. **(F)** From left to right, boxplots of spreading size, measured within the boundary defined by the stress fibers. Strain energy, calculated by summing up the squared scalar product of traction force and displacement field divided by two. σ_{xx} and σ_{yy} calculated by averaging the stress maps obtained with monolayer stress microscopy. Degree of polarization, defined as the difference of the average σ_{xx} - and σ_{yy} -stress normalized by their sum. Doublets are shown in yellow and singlets are shown in green. The figure shows data from $n = 106$ doublets from $N = 10$ samples and $n = 72$ singlets from $N = 12$ samples. All scale bars are $10\ \mu\text{m}$ long.

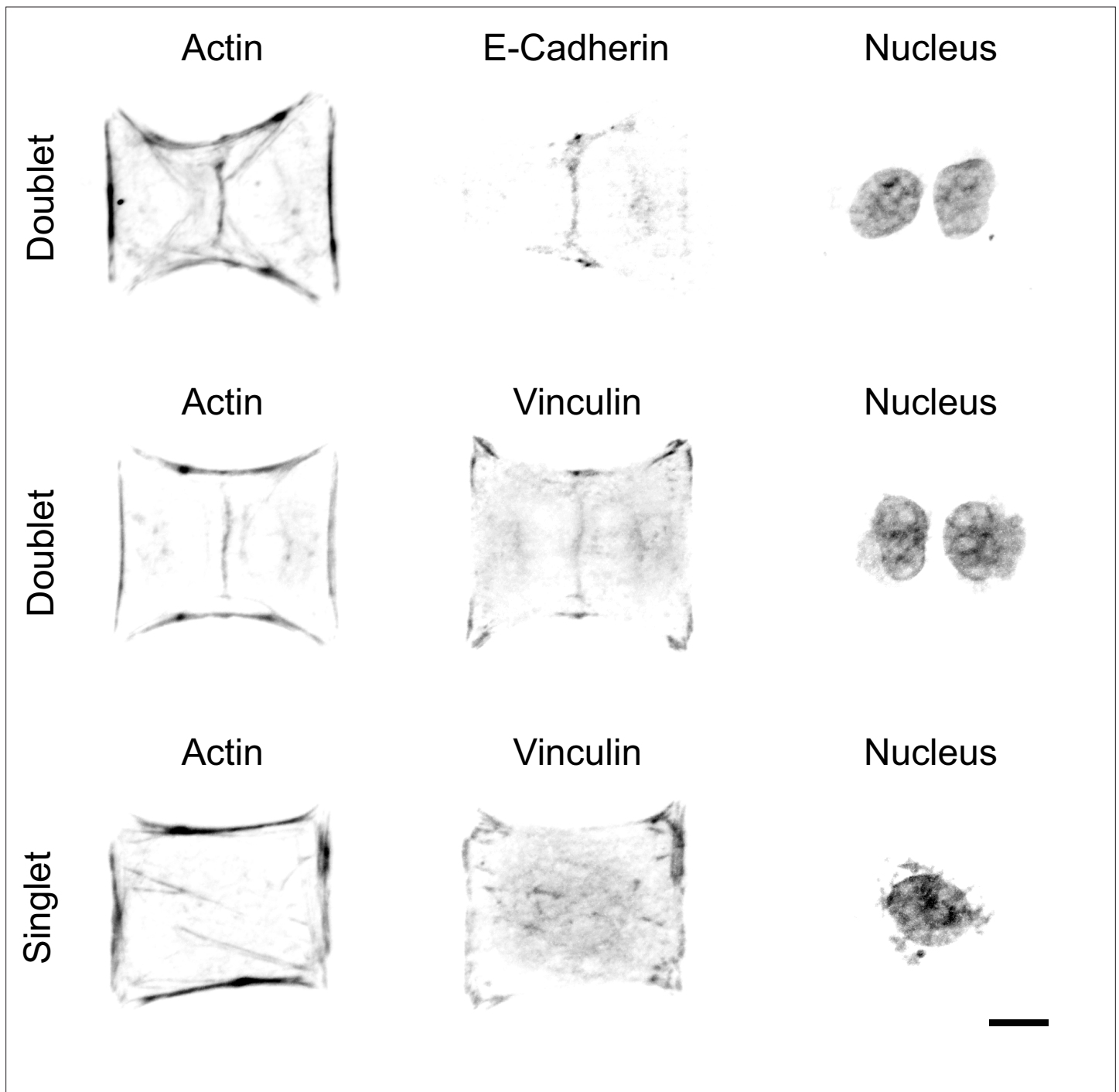


Figure 1—figure supplement 1. Immunostaining of opto-MDCK cells plated on H-patterns and incubated for 24 hr before fixing. Actin, E-cadherin, vinculin, and the nucleus are shown. The top and middle rows show a representative example of a doublet, and the bottom row shows a representative example of a singlet. Scale bar is 10 μm long.

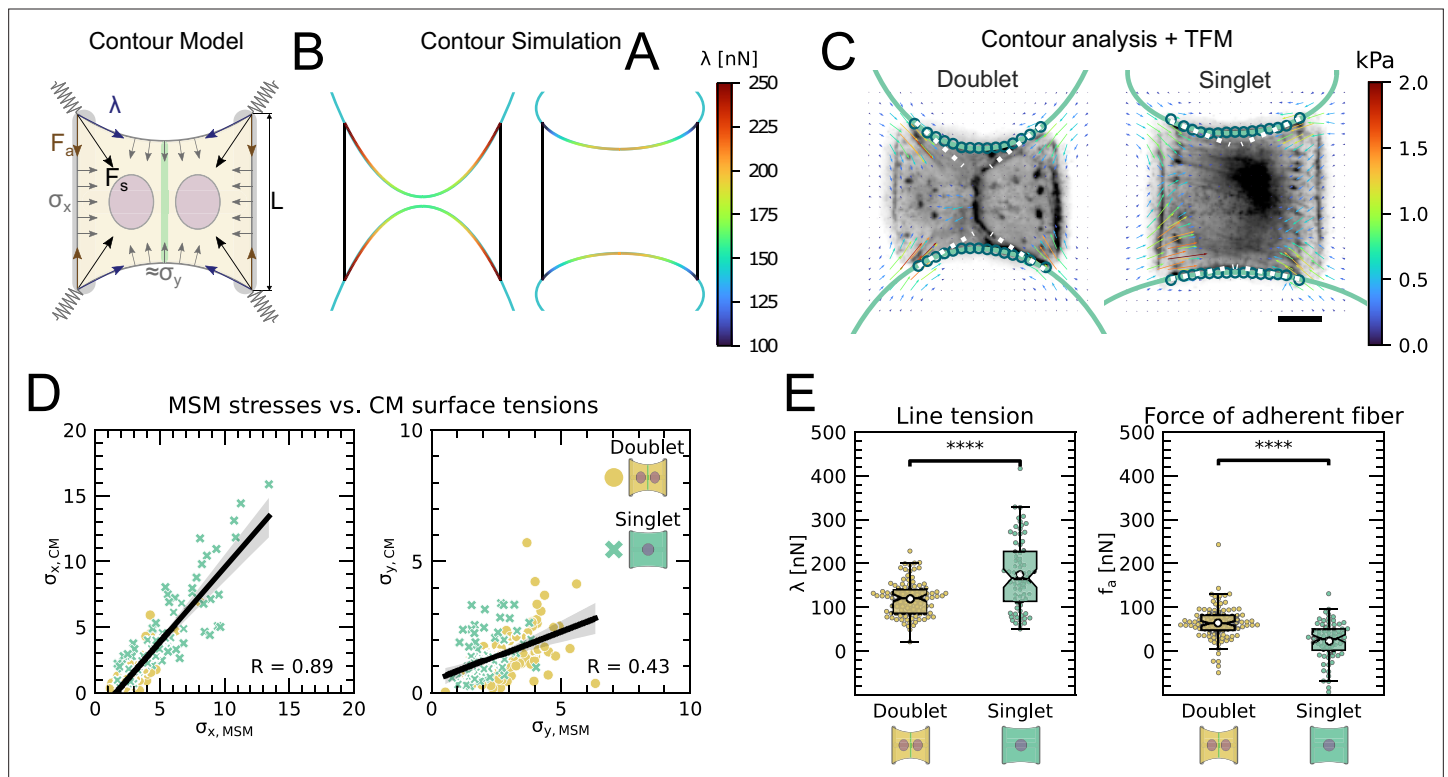


Figure 2. The cell–cell junction leads to a redistribution of tension from free to adherent peripheral stress fiber. **(A)** Cartoon of the contour model used to analyze the shape of the doublets and singlets. **(B)** Finite element method (FEM) simulation of the contour with $\sigma_y > \sigma_x$ left and $\sigma_x > \sigma_y$ right. **(C)** Actin images of doublets (left) and singlets (right) with traction stresses (arrows), tracking of the free fiber (blue circles), elliptical contour fitted to the fiber tracks (green line), and tangents to the contour at adhesion point (white dashed line). The scale bar is $10\ \mu\text{m}$ long. **(D)** Correlation plot of monolayer stress microscopy (MSM) stresses and CM surface tensions. MSM stresses were calculated by averaging the stress maps obtained with monolayer stress microscopy, and the surface tensions were obtained by the contour model analysis, where σ_x was measured on the traction force microscopy (TFM) maps by summing up the x-traction stresses in a window around the center of the vertical fiber and σ_y was determined by fitting the resulting ellipse to the tracking data of the free fiber. Doublets are shown as yellow dots, and singlets are shown as green crosses. The black line shows the linear regression of the data, and the shaded area shows the 95% confidence interval for this regression. The R-value shown corresponds to the Pearson correlation coefficient. **(E)** Boxplots of line tension λ (left) and force of adherent fiber F_a (right) as defined in panel (A). Both values were calculated by first calculating the force in each corner by summing up all forces in a radius of $12\ \mu\text{m}$ around the peak value and then projecting the resulting force onto the tangent of the contour for the line tension and onto the y-axis for the force of adherent fiber. Doublets are shown in yellow, and singlets are shown in green. The figure shows data from $n = 106$ doublets from $N = 10$ samples and $n = 72$ singlets from $N = 12$ samples. All scale bars are $10\ \mu\text{m}$ long.

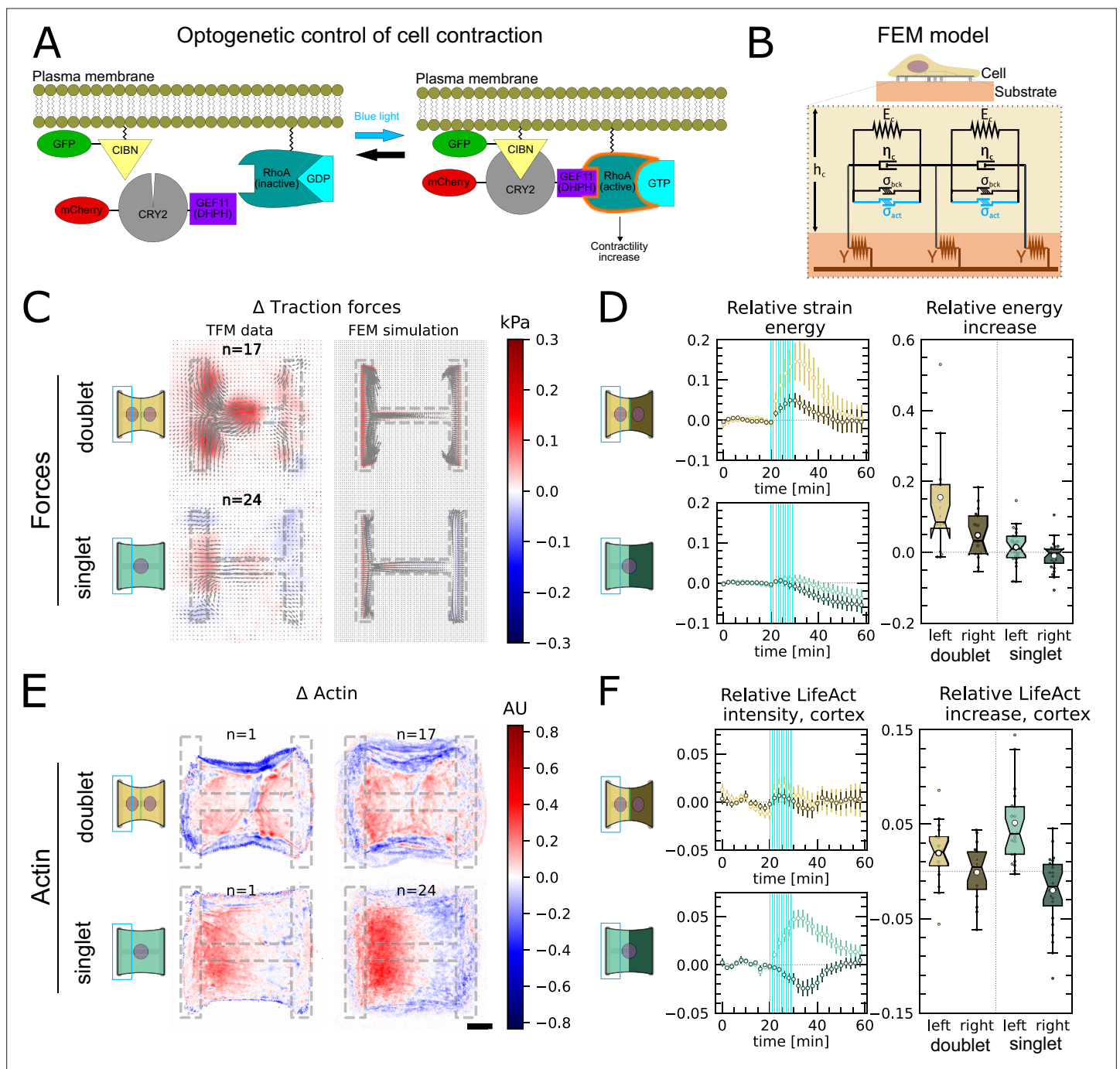


Figure 3. Local activation of RhoA leads to stable force increase in both the activated and the nonactivated cell in doublets, but destabilizes force homeostasis in singlets. **(A)** Cartoon of the optogenetic CIBN/CRY2 construction used to locally activate RhoA. **(B)** Cartoon of the FEM continuum model used to explain optogenetic experiments. **(C)** Difference of average traction force maps after and before photoactivation of cell doublets (top) and singlets (bottom). Maps on the left show the traction force microscopy (TFM) data, and maps on the right show the result of the FEM simulations with an active response of the right cell. **(D)** Relative strain energies of doublets (top) and singlets (bottom) with local photoactivation, divided into left half (bright) and right half (dark). One frame per minute was acquired for 60 min, and cells were photoactivated with one pulse per minute for 10 min between minute 20 and minute 30. Strain energy curves were normalized by first subtracting the individual baseline energies (average of the first 20 min) and then dividing by the average baseline energy of all cell doublets/singlets in the corresponding datasets. Data is shown as circles with the mean \pm SEM. Boxplots on the right show the value of the relative strain energy curves 2 min after photoactivation, that is, at minute 32. **(E)** Difference of actin images after and before photoactivation of doublets (top) and singlets (bottom), with an example on the left and the average on the bottom. All scale bars are $10\ \mu\text{m}$ long. **(F)** LifeAct intensity measurement inside the cells over time (left) of left half (bright) vs. right half (dark) of doublets (top) and singlets (bottom) after local photoactivation. Boxplots on the right show the relative actin intensity value after 2 min after photoactivation of activated vs. nonactivated half. The figure shows data from $n = 17$ doublets from $N = 2$ samples and $n = 17$ singlets from $N = 6$ samples. All scale bars are $10\ \mu\text{m}$ long.

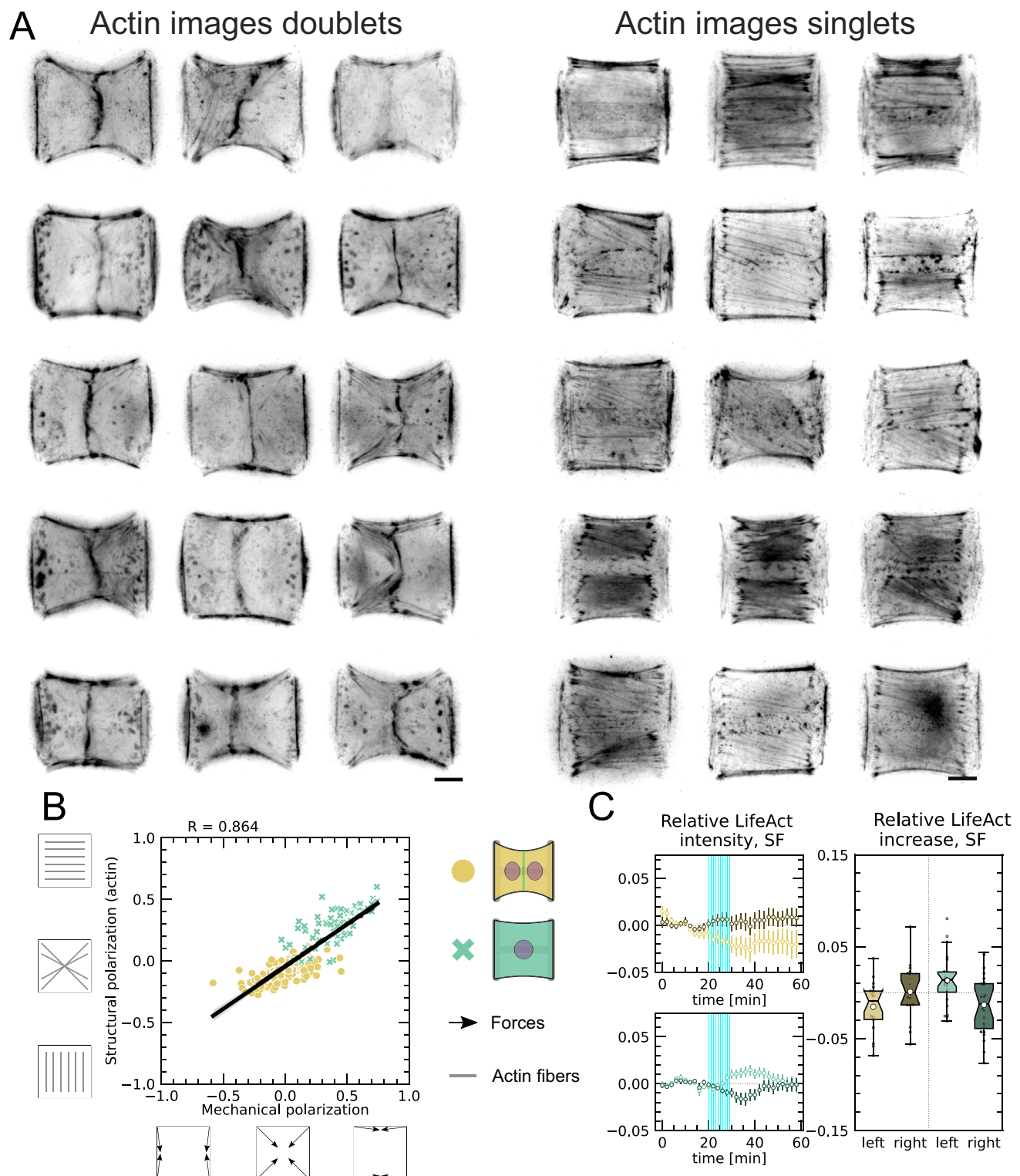


Figure 3—figure supplement 1. LifeAct images of doublets and singlets on H-patterns, quantification of mechano-structural polarization and measurement of LifeAct intensities of stress fibers in response to optogenetical activation of RhoA. **(A)** LifeAct images of some example opto-MDCK doublets (left) and singlets (right) plated on H-patterns. **(B)** Correlation plot of mechanical and structural polarization. The black line shows the linear regression of the data, and the shaded area shows the 95% confidence interval for this regression. The R-value shown corresponds to the Pearson correlation coefficient. **(C)** Relative LifeAct intensity of stress fibers (SF) in response to optogenetical activation of RhoA. The left graph shows the relative LifeAct intensity of stress fibers over time. The right graph shows the relative LifeAct increase of stress fibers over time. The box plot on the right shows the distribution of relative LifeAct increase of stress fibers for doublets (left) and singlets (right) before and after activation.

Figure 3—figure supplement 1 continued on next page

Figure 3—figure supplement 1 continued

correlation coefficient. Scale bar is 10 μm long. (C) LifeAct intensity measurement on periphery of cells over time (left) of left half (bright) vs. right half (dark) of doublets (top) and singlets (bottom) after local photoactivation. Boxplots on the right show the relative actin intensity value after 2 min after photoactivation of activated vs. nonactivated half.

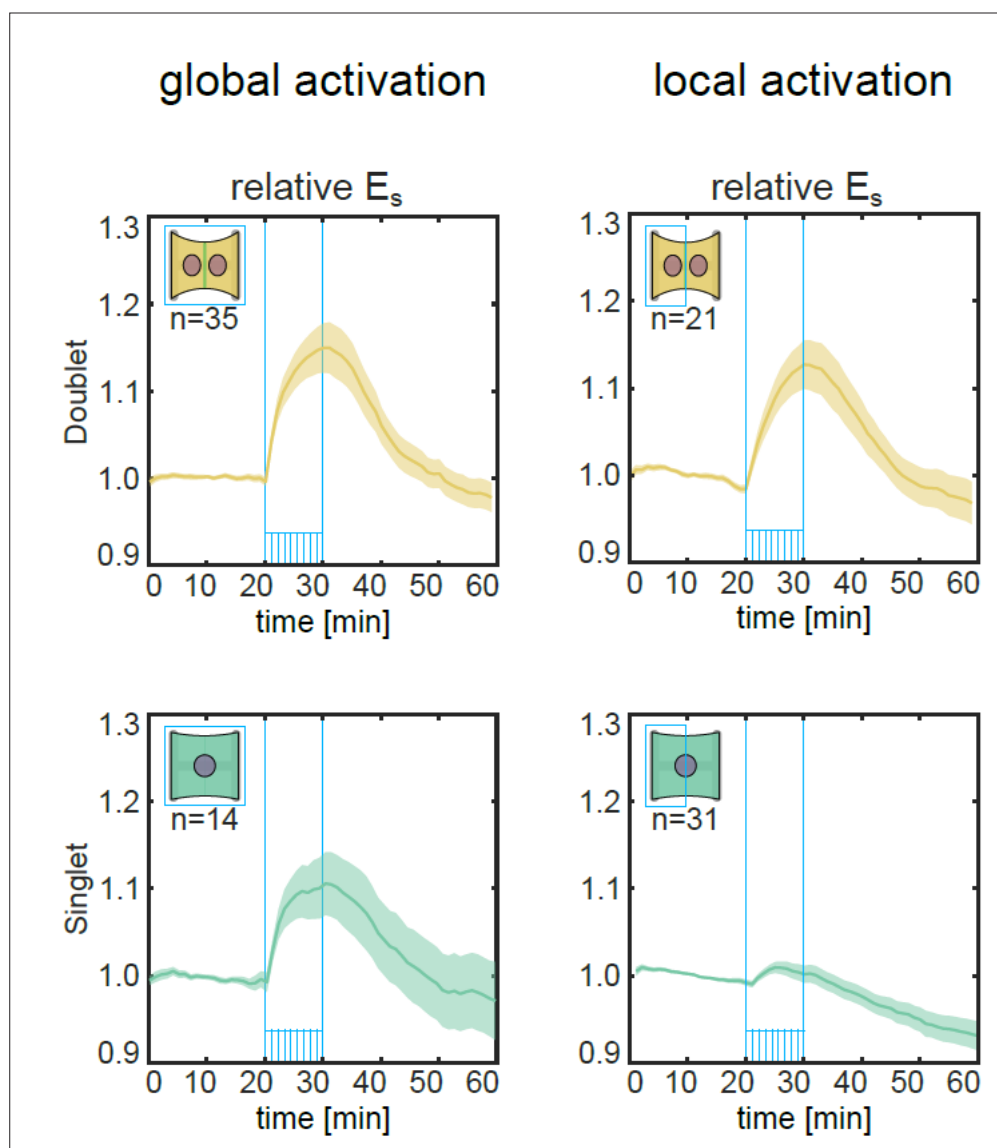


Figure 3—figure supplement 2. Relative strain energies of local (left) vs. global (right) photoactivation of doublets (top) and singlets (bottom).

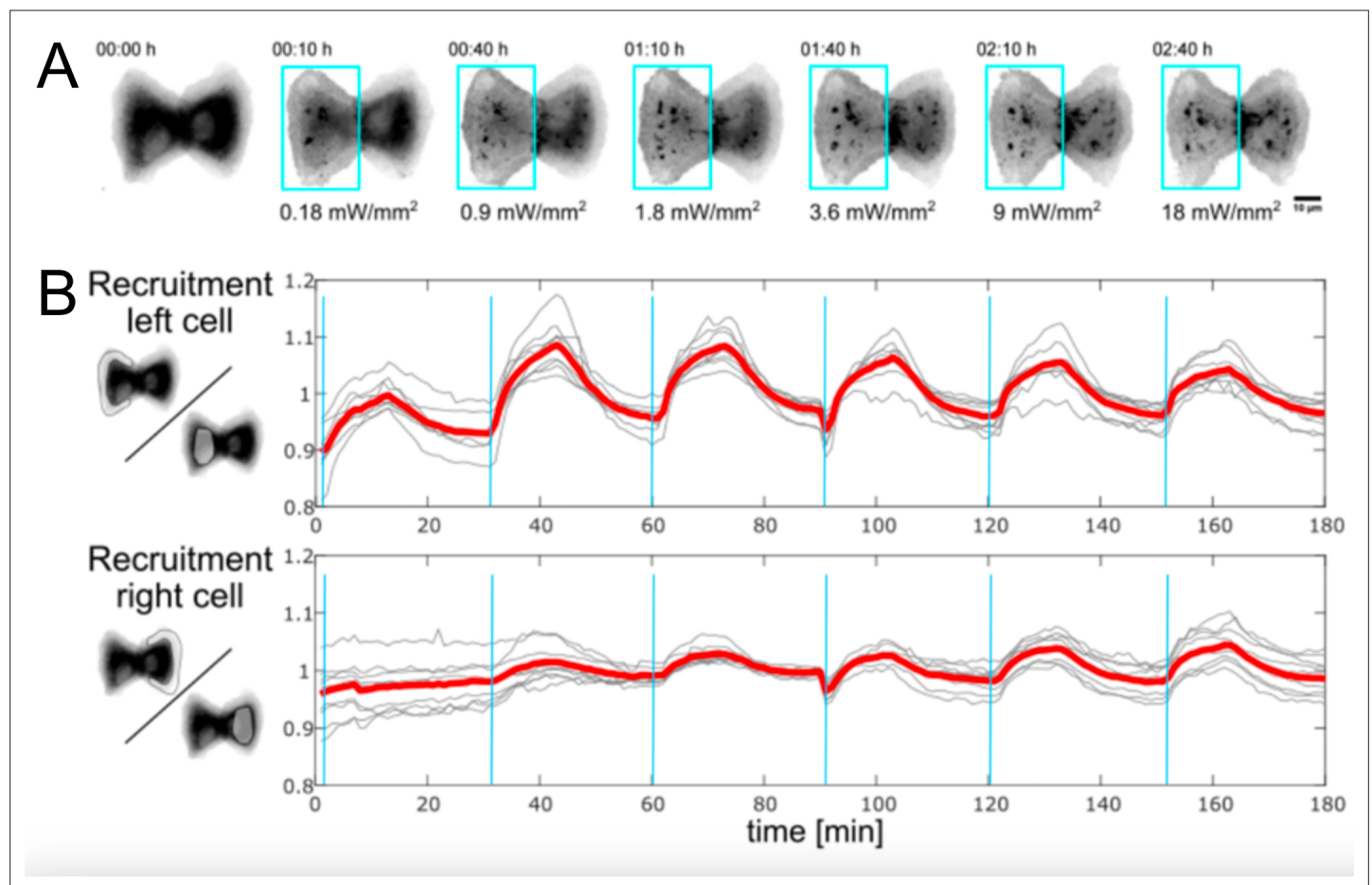


Figure 3—figure supplement 3. Recruitment of CRY2 to the membrane in left vs. right cell in response to optogenetic activation with varying light intensities. (A) Fluorescence images of CRY2 in MDCK cell doublets in response to photoactivation pulse of increasing power. (B) CRY2 recruitment from the cytosol to the plasma membrane, quantified by measuring the ratio of intensities in the lamellipodium vs. the cytosol.

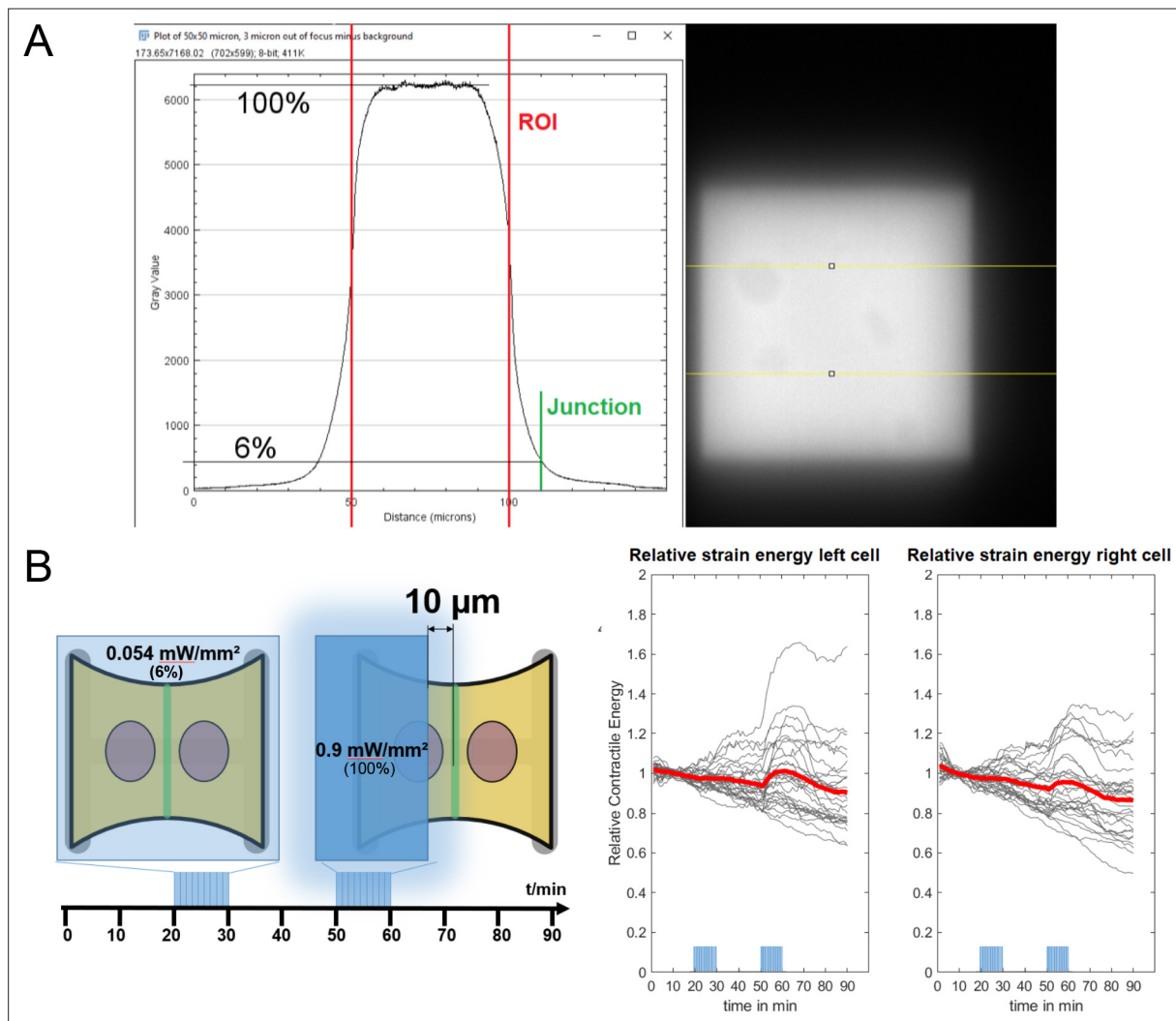


Figure 3—figure supplement 4. Strain energy increase of non-activated cell is not caused by accidental photoactivation through stray light. **(A)** Fluorescence image of a homogeneously coated coverslip, illuminated on a rectangular zone with a digital micromirror device (DMD) and the horizontal intensity profile. The background was subtracted from the image before making the measurements. The peak intensity drops to 6% over a distance of 10 μm, so all local activation routines were placed 10 μm away from the junction. **(B)** Left: a cartoon describing the experiment. First, the whole doublet is activated at low light intensity (0.054 mW mm⁻²) and then only the left cell is activated with higher intensity (0.9 mW mm⁻²). The intensity of the first activation routine corresponds to the intensity right at the junction from the second activation routine. Right: curves show the strain energy stored in the substrate under the left cell (left) and under the right cell (right). The strain energy curves were normalized by the strain energy level before photoactivation. Red curves show the average, and gray curves show the individual doublets.

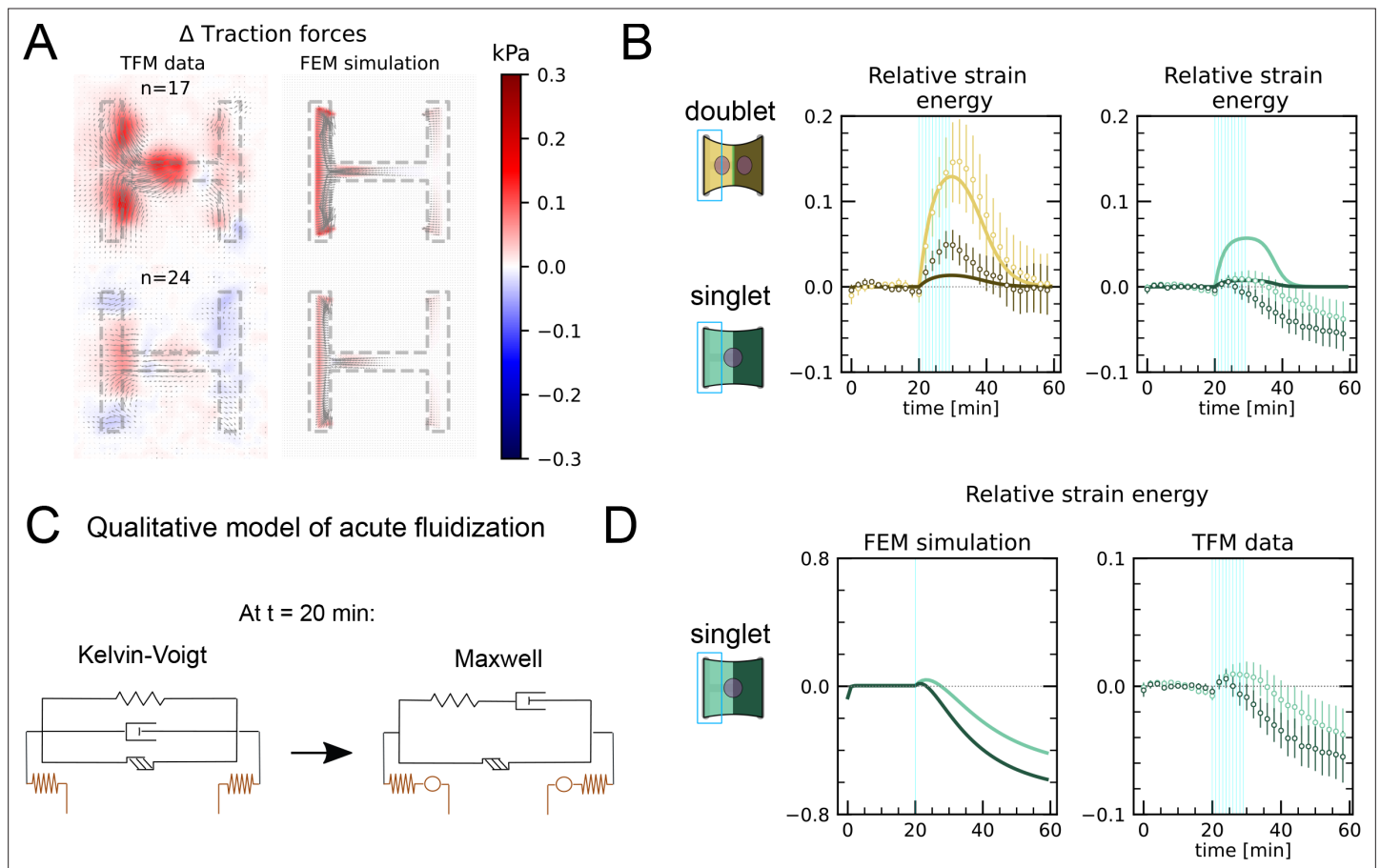


Figure 3—figure supplement 5. Acute fluidization of actin structures in singlets is a plausible explanation of the observed strain energy curves in response to local optogenetic activation of RhoA. **(A)** Difference of average traction force maps after and before photoactivation of cell doublets (top) and singlets (bottom). Maps on the left show the traction force microscopy (TFM) data and maps on the right show the result of the FEM simulations without any active reaction of the right cell. **(B)** Relative strain energies of doublets (top) and singlets (bottom) with local photoactivation, divided in left half (bright) and right half (dark). One frame per minute was acquired for 60 min, and cells were photoactivated with one pulse per minute for 10 min between minute 20 and minute 30. Strain energy curves were normalized by first subtracting the individual baseline energies (average of the first 20 min) and then dividing by the average baseline energy of all cell doublets/singlets in the corresponding datasets. Data is shown as circles with the mean \pm SEM, and simulated curves are shown as solid lines. **(C)** A cartoon showing the basic elements of the FEM simulation. Acute fluidization is modeled as a switch from Kelvin-Voigt to Maxwell elements. **(D)** Relative strain energies of singlets with local photoactivation, divided in left half (bright) and right half (dark). One frame per minute was acquired for 60 min, and cells were photoactivated with one pulse per minute for 10 min between minute 20 and minute 30. Strain energy curves were normalized by first subtracting the individual baseline energies (average of the first 20 min) and then dividing by the average baseline energy of all cell doublets/singlets in the corresponding datasets. Data is shown as circles with the mean \pm SEM, and the result of an FEM simulation is shown as a solid line.

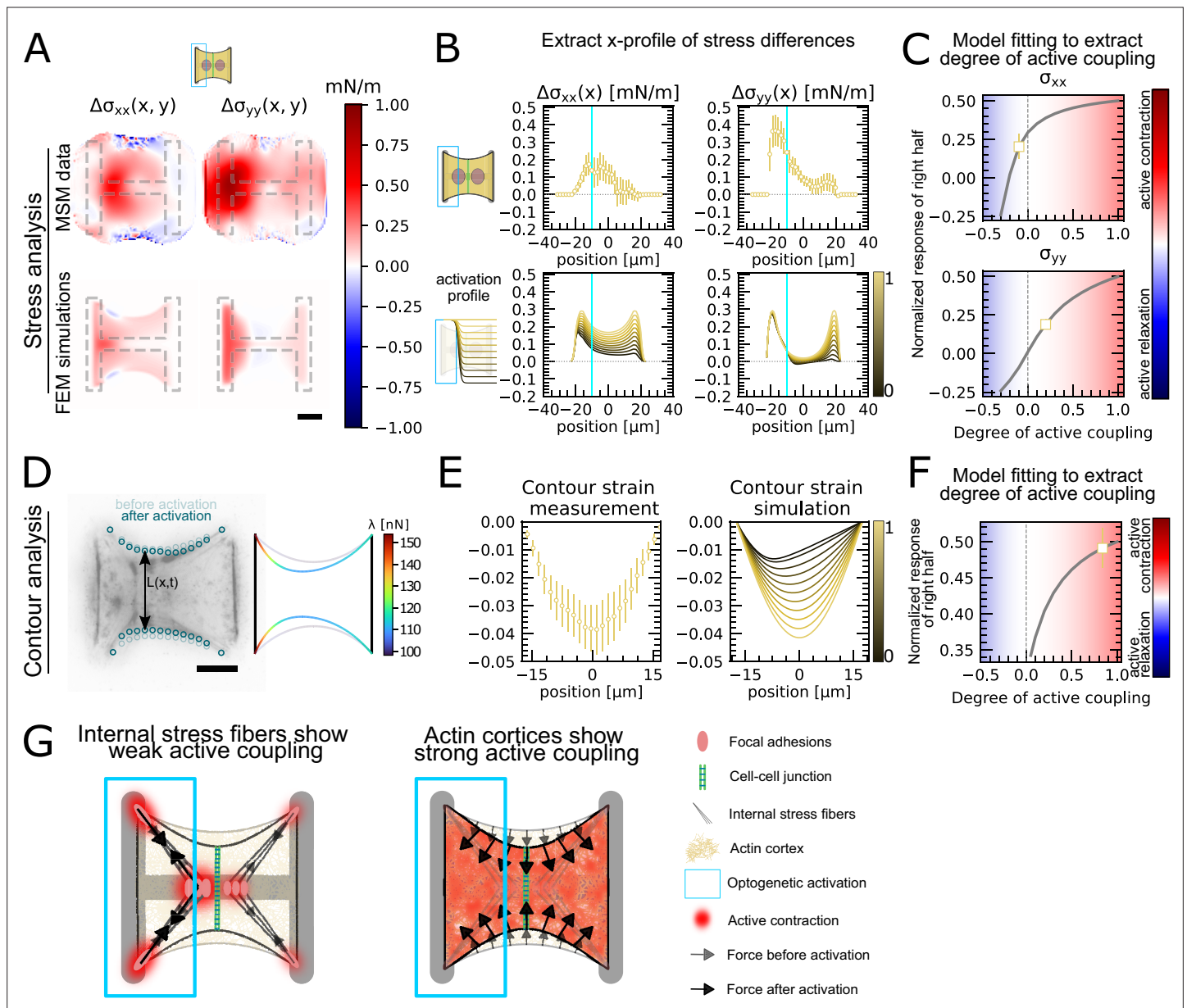


Figure 4. Stress and contour modeling shows strong active coupling of actin cortices in doublets. **(A)** Difference of average cell stress maps after and before photoactivation of cell doublets, calculated with monolayer stress microscopy (MSM) (top) and simulated with the FEM continuum model (bottom). Stress in x-direction is shown on the left, and stress in y-direction is shown on the right. **(B)** Average over the y-axis of the maps in **(A)**. Data is shown as circles with the mean \pm SEM. In the simulation, the right half of the cell was progressively activated to obtain the family of curves shown in the bottom. **(C)** Response of the right half (normalized by the total response), obtained from the model (gray line), as a function of the degree of active coupling. The experimental MSM value is placed on the curve to extract the degree of active response of the right cell in the experiment. **(D)** Contour analysis of the free stress fiber. In the experiment, the distance between the free fibers as a function of x is measured, as shown in the image on the left. An example for a contour model simulations is shown in the right. **(E)** The contour strain after photoactivation is calculated from the distance measurements shown in **(D)** by dividing the distance between the free stress fibers for each point in x -direction after and before photoactivation. Similarly to the FEM simulation, in the contour simulation, the right half of the contour is progressively activated to obtain the curve family shown in the right plot. **(F)** Response of the right half (normalized by the total response), obtained from the model (gray line), as a function of the degree of active coupling. The experimental strain value is placed on the curve to extract the degree of active response of the right cell in the experiment. **(G)** A cartoon showing our interpretation of the results shown in panels **(A–F)**. The traction force analysis only measures forces that are transmitted to the substrate, which are dominated by the activity of the stress fibers. The contour of the free fiber is determined by the activity of the actin cortex and the free stress fiber. Thus, the strong active coupling in the contour suggests strong active coupling of the cortices and the comparatively weak active coupling of the forces suggests a weak active coupling of the stress fibers. The figure shows data from $n = 17$ doublets from $N = 2$ samples. All scale bars are $10 \mu\text{m}$ long.

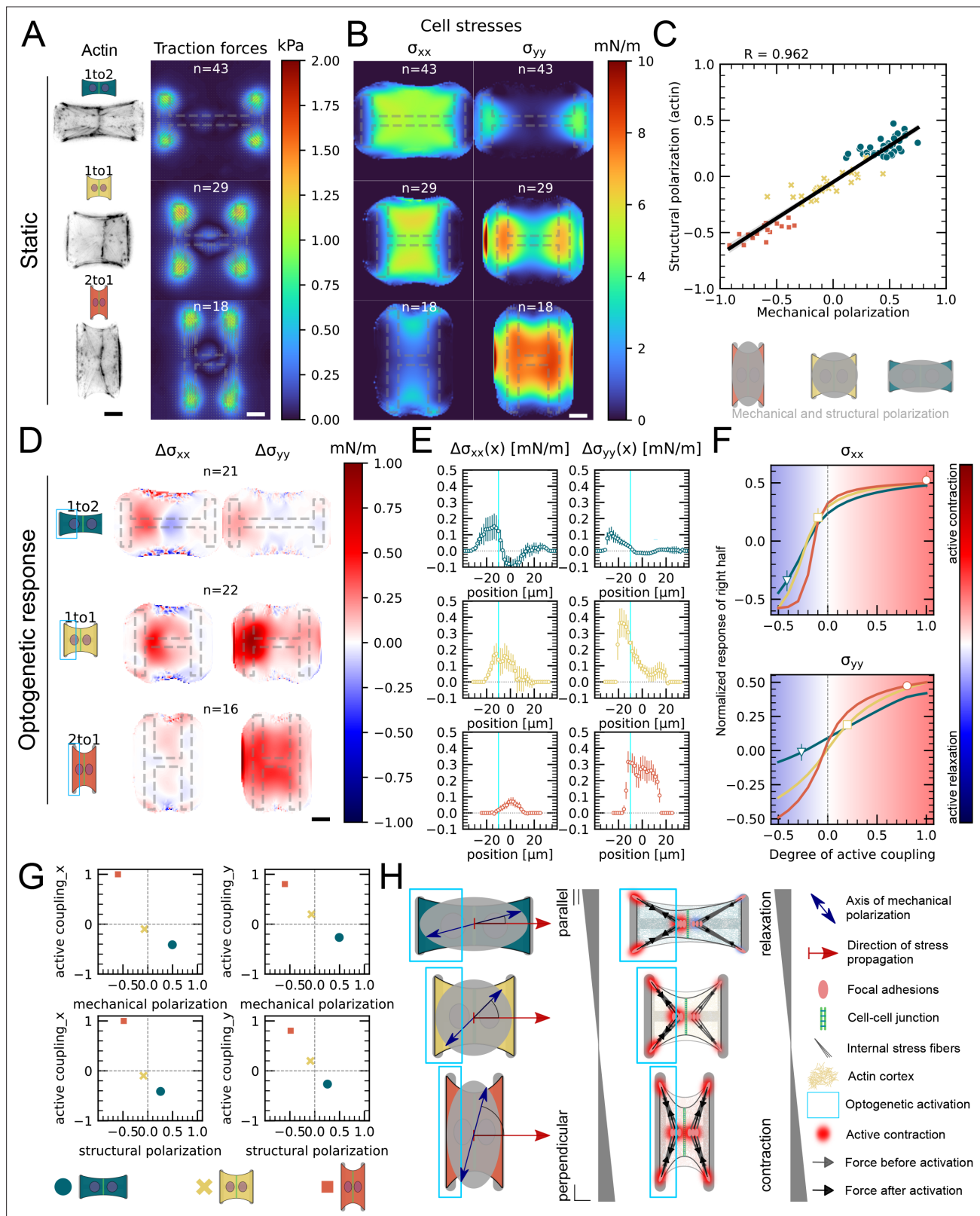


Figure 5. Mechanical stresses transmit most efficiently perpendicularly to the axis of mechanical and structural polarization in doublets. **(A)** Actin images (left) and average traction stress and force maps (right) of cell doublets on H-patterns with different aspect ratios (1 to 2, 1 to 1, and 2 to 1). **(B)** Average cell stress maps calculated by applying a monolayer stress microscopy algorithm to the traction stress maps. **(C)** Correlation plot of mechanical and structural polarization. The black line shows the linear regression of the data, and the shaded area shows the 95% confidence interval for this regression.

Figure 5 continued on next page

Figure 5 continued

The R-value shown corresponds to the Pearson correlation coefficient. **(D)** Stress maps of the difference of xx-stress (left) and yy-stress (right) before and after photoactivation. **(E)** Average over the y-axis of the maps in **(D)**. Data is shown as circles with the mean \pm SEM. **(F)** Response of the right half (normalized by the total response), obtained from the model (gray line), as a function of the degree of active coupling. The experimental monolayer stress microscopy (MSM) value is placed on the curve to extract the degree of active response of the right cell in the experiment. All scale bars are 10 μm long. **(G)** The degree of active coupling plotted against the average mechanical and structural polarization. **(H)** A cartoon showing our interpretation of the data shown in panels **(A–F)**. The relative response of the right cell in response to the activation of the left cell varies strongly in the different aspect ratios. In the 1 to 2 doublet, where polarization and transmission direction are aligned, the right cell relaxes, whereas in the 2 to 1 doublet, where the polarization axis is perpendicular to the transmission direction, the right cell contracts almost as strongly as the left cell. The figure shows data from $n = 43$ 1 to 2 doublets from $N = 6$ samples, $n = 29$ 1 to 1 doublets from $N = 2$ samples, and $n = 18$ 2 to 1 doublets from $N = 3$ samples. For the analysis of the optogenetic data, doublets with unstable stress behavior before photoactivation were excluded. All scale bars are 10 μm long.

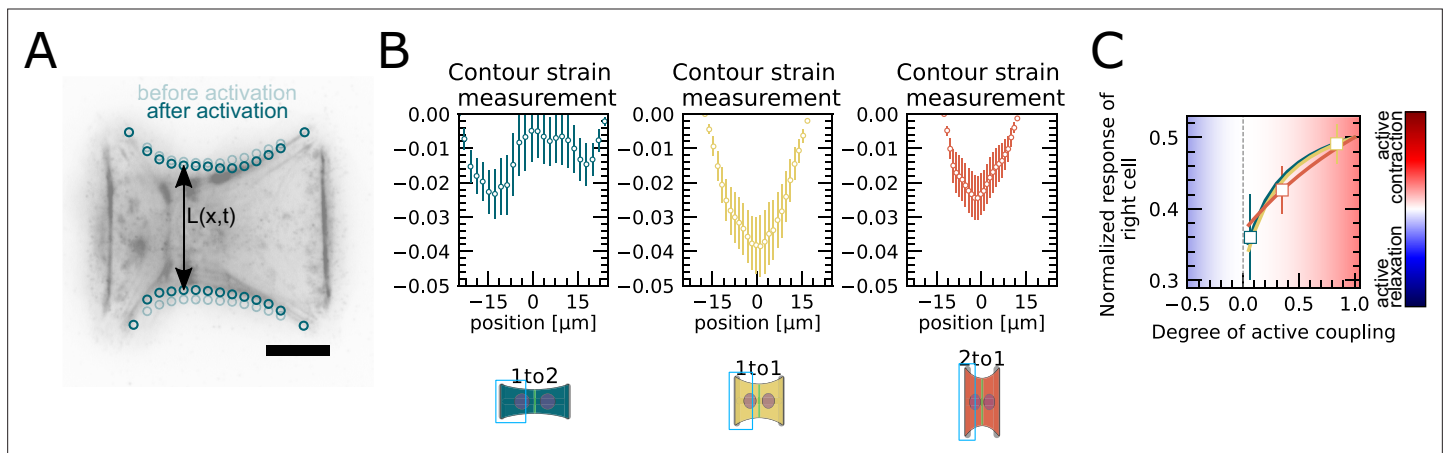


Figure 5—figure supplement 1. Contour strain measurements of doublets with varying aspect ratios. **(A)** Contour analysis of the free stress fiber. In the experiment, the distance between the free fibers as a function of x is measured, as shown in the image on the left. **(B)** The contour strain after photoactivation is calculated from the distance measurements shown in **(A)**, by dividing the distance between the free stress fibers for each point in x -direction after and before photoactivation. **(C)** Response of the right half (normalized by the total response), obtained from the model (solid lines), as a function of the degree of active coupling. The experimental strain value is placed on the curve to extract the degree of active response of the right cell in the experiment.

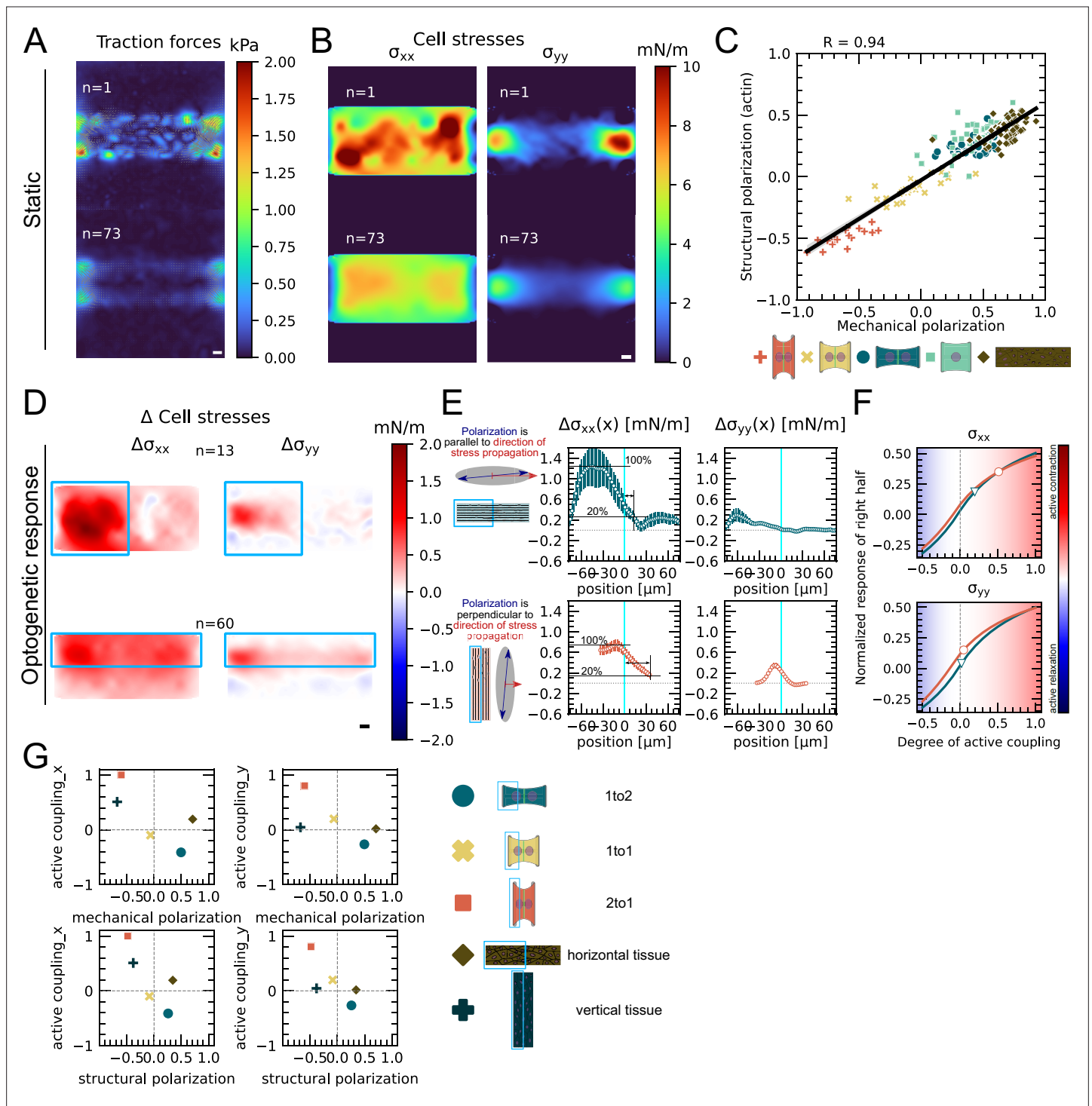


Figure 6. Mechanical stresses transmit most efficiently perpendicularly to the axis of mechanical and structural polarization in small monolayers. **(A)** Representative (top) and average (bottom) maps of traction forces and stresses of a small monolayer on rectangular micropattern. **(B)** Representative example and average cell stress maps calculated by applying a monolayer stress microscopy algorithm to the traction stress maps. **(C)** Correlation plot of mechanical and structural polarization across all conditions. The black line shows the linear regression of the data, and the shaded area shows the 95% confidence interval for this regression. The R-value shown corresponds to the Pearson correlation coefficient. **(D)** Stress maps of the difference of xx-stress (left) and yy-stress (right) before and after photoactivation. **(E)** Average over the y-axis of the maps in **(D)**. Data is shown as circles with the mean \pm SEM. **(F)** Response of the right half (normalized by the total response), obtained from the model (gray line), as a function of the degree of active coupling. The experimental monolayer stress microscopy (MSM) value is placed on the curve to extract the degree of active response of the right cell in the experiment. **(G)** The degree of active coupling plotted against the average mechanical and structural polarization. All scale bars are 10 μm long. The Figure 6 continued on next page

Figure 6 continued

figure shows data from $n = 13$ tissues from $N = 2$ samples photoactivated on the left and from $n = 60$ tissues from $N = 3$ samples photoactivated on the top. All scale bars are $10\ \mu\text{m}$ long.

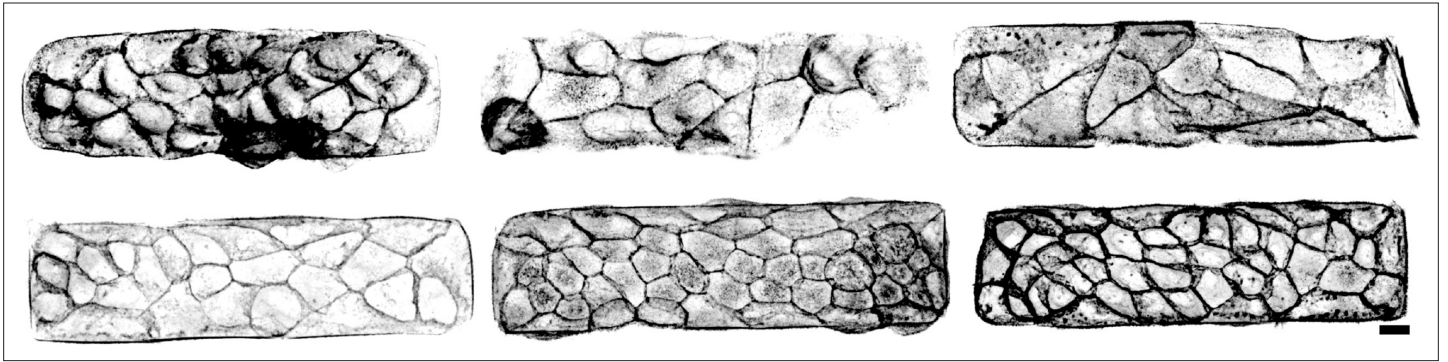
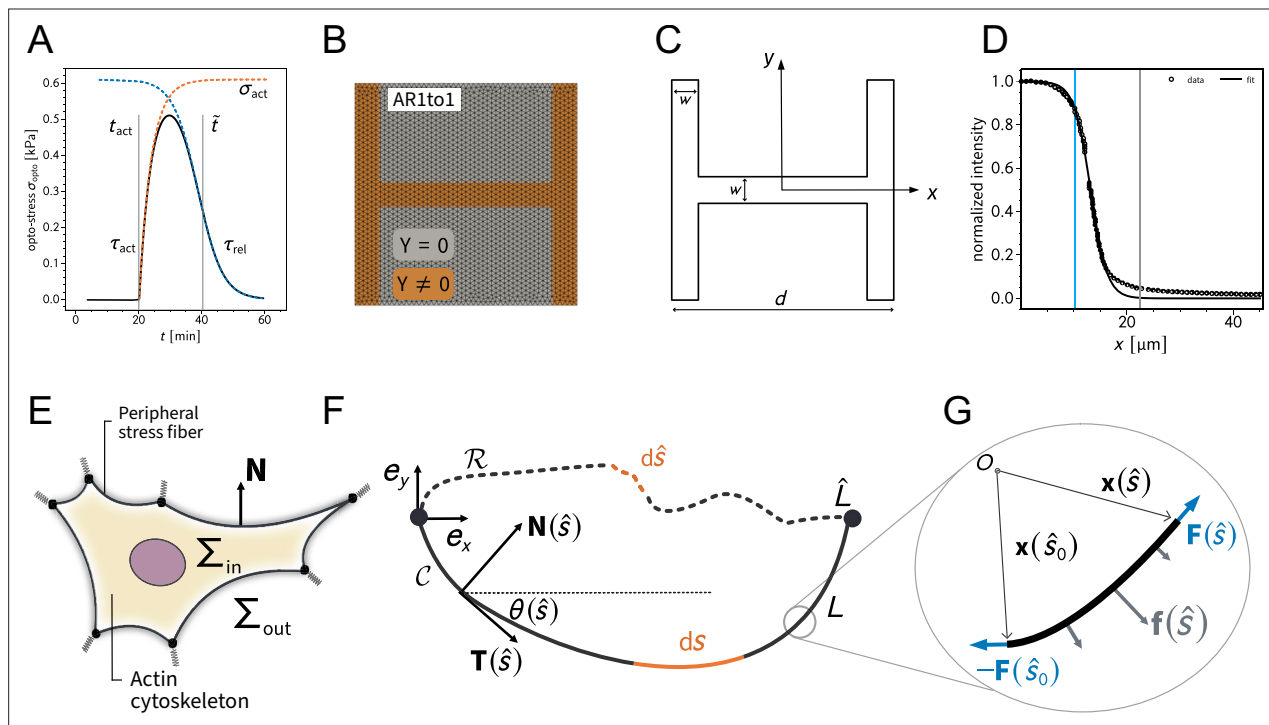
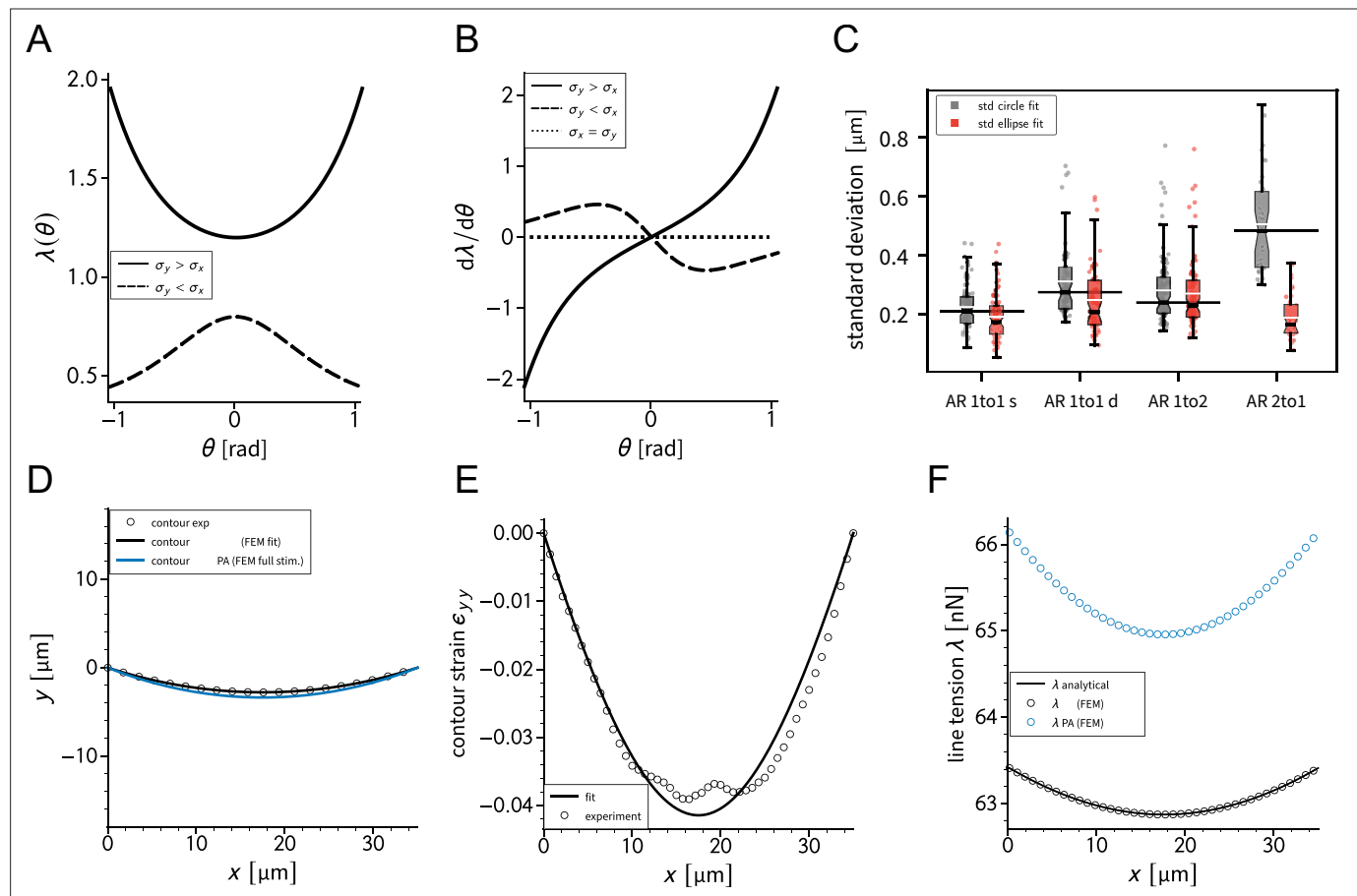


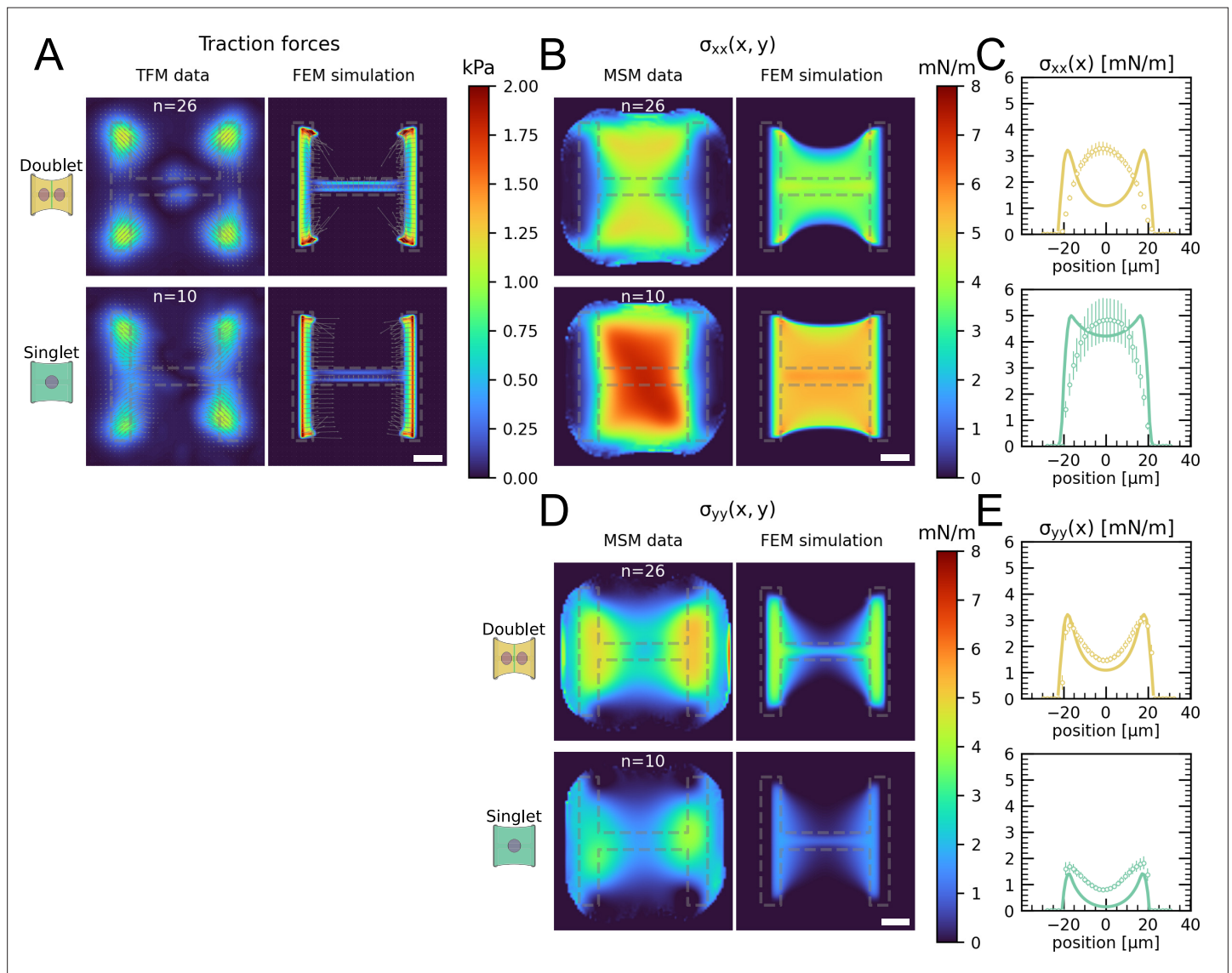
Figure 6—figure supplement 1. Phalloidin stainings of actin structures of small tissues. Scale bar is 10 μm long.



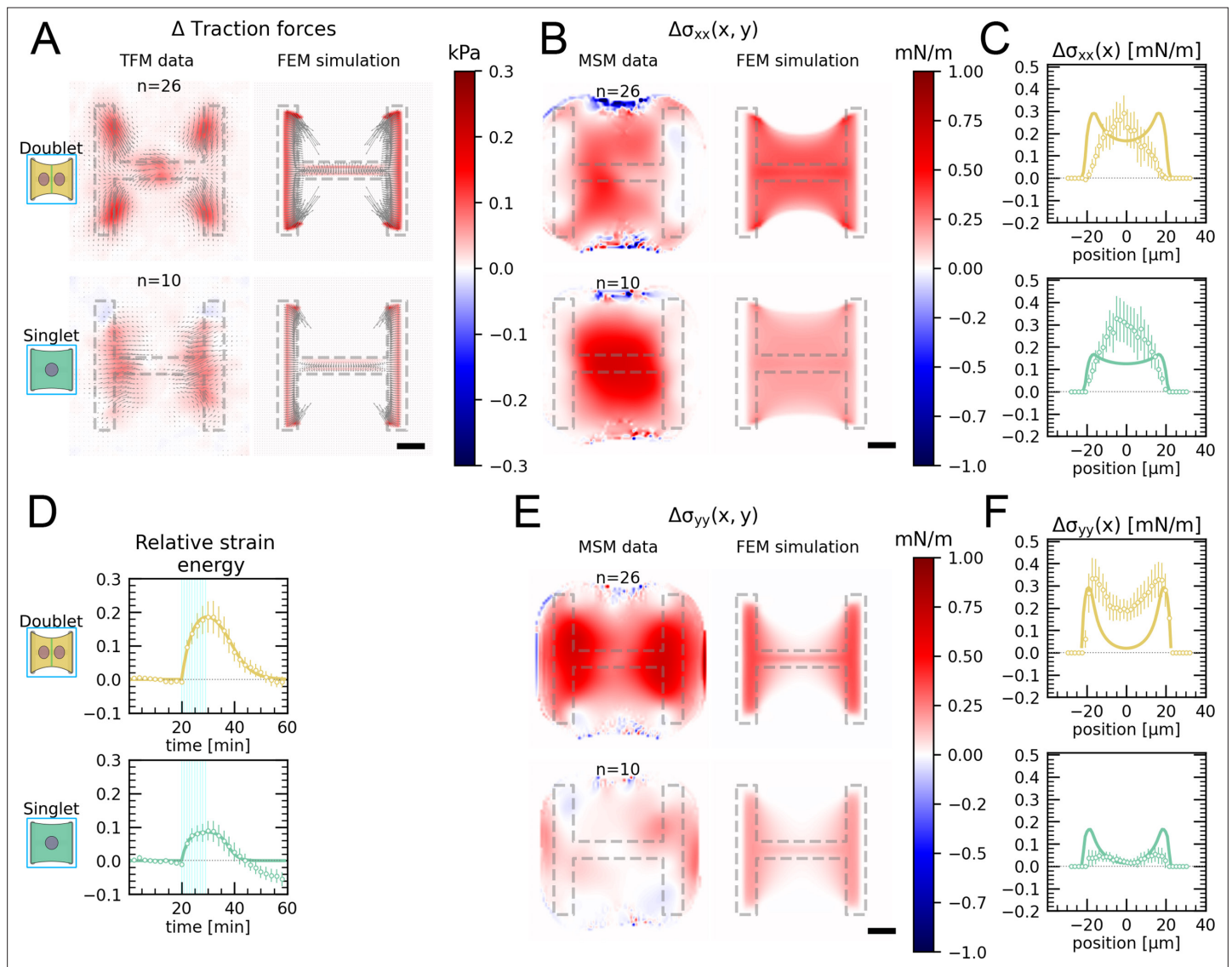
Appendix 1—figure 1. Overview of the 2D finite element simulation and the notation for the contour model. (A) shows the shape of the by optogenetic-induced time-dependent stress. (B) depicts the finite element mesh created with GMSH. The spring stiffness density is nonzero on the brown part of the domain. (C) is a schematic illustration of the relevant parameters to define the adhesion geometry. (D) shows the experimentally measured intensity profile of the light pulse used for photoactivation. The gray line indicates the center of the pattern (measured from left to right) while the blue line marks the inflection point of the sigmoidal fit function. (E) is a schematic illustration of the relevant quantities in the contour-based description of cellular adhesion. (G, F) explain the relevant mathematical quantities to describe the equilibrium shape of a fiber subject to external loads.



Appendix 1—figure 2. Calibration check for the contour model. (A, B) show the predicted line tensions and the derivative with respect to the turning angle based on the analytical solution for different values of σ_x and σ_y . (C) compares the circle and ellipse fit of the contour of the cells for different pattern aspect ratios. (D) shows a generic cell contour for the doublet before and during photo-activation. The experimentally contour strain in y -direction with the respective fit from simulations and the corresponding line tensions are shown in (E) and (F), respectively.



Appendix 1—figure 3. Comparison of traction forces and stress distribution between experiment and finite element simulation. **(A)** Average traction stress and force maps of cell doublets (top) and singlets (bottom) on H-patterns on the left and corresponding traction stress and force maps from the FEM simulation. **(B, D)** Average cell stress maps of cell doublets (top) and singlets (bottom) on H-patterns on the left and corresponding cell stress maps from the FEM simulation. **(C, E)** Average over the y-axis of the maps in **(B)** and **(D)**. Data is shown as circles with the mean \pm SEM, the solid line corresponds to the FEM simulations. All scale bars are $10 \mu\text{m}$ long.



Appendix 1—figure 4. Comparison of traction forces stress distribution and strain energy between experiment and finite element simulation for global photoactivation. **(A)** Average traction stress and force map difference before and after photoactivation of cell doublets (top) and singlets (bottom) on H-patterns on the left and corresponding traction stress and force maps from the FEM simulation. **(B, E)** Average cell stress map difference before and after photoactivation of cell doublets (top) and singlets (bottom) on H-patterns on the left and corresponding cell stress maps from the FEM simulation. **(C, F)** Average over the y-axis of the maps in **(B)** and **(D)**. Data is shown as circles with the mean \pm SEM, the solid line corresponds to the FEM simulations. **(D)** Relative strain energies of doublets (top) and singlets (bottom) with global photoactivation. One frame per minute was acquired for 60 min, and cells were photoactivated with one pulse per minute for 10 min between minute 20 and minute 30. Strain energy curves were normalized by first subtracting the individual baseline energies (average of the first 20 min) and then dividing by the average baseline energy of all cell doublets/singlets in the corresponding datasets. Data is shown as circles with the mean \pm SEM, and the result of an FEM simulation is shown as a solid line. All scale bars are 10 μ m long.